Regional Dependence of Seismic Migration Patterns

Yi-Hsuan Wu[1, *], Chien-Chih Chen[2], John B. Rundle[3], and Jeen-Hwa Wang[1]

[1] *Institute of Earth Sciences, Academia Sinica, Taipei, Taiwan, ROC*
[2] *Department of Earth Sciences and Graduate Institute of Geophysics, National Central University, Jhongli, Taiwan, ROC*
[3] *Center for Computational Sciences and Engineering, UC Davis, Davis, CA, USA*

ABSTRACT

In this study, we used pattern informatics (PI) to visualize patterns in seismic migration for two large earthquakes in Taiwan. The 2D PI migration maps were constructed from the slope values of temporal variations of the distances between the sites and hotspot recognized from the PI map. We investigated the 2D PI migration pattern of the 1999 Chi-Chi and 2006 Pingtung earthquakes which originated from two types of seismotectonic setting. Our results show that the PI hotspots migrate toward the hypocenter only when the PI hotspots are generated from specific depth range which is associated with the seismotectonic setting. Therefore, we conclude that the spatiotemporal distribution of events prior to an impending earthquake is significantly affected by tectonics.

1. INTRODUCTION

To mitigate seismic risks, predicting or forecasting an impending earthquake is a serious challenge in seismology. To gain insight into earthquake physics, dynamical models (cf. Main 1996; Wang 2008) and statistical physics methods (cf. Main 1996) have been used to study seismicity and related phenomena, including quiescence, activation, and migration, prior to large impending earthquakes. Without knowledge of the underlying dynamics, it is difficult to comprehensively understand such behavior. Studying anomalous seismicity related to precursor processes for large earthquakes using statistical methods can help understand how large earthquakes are initiated. Among the statistical physics methods (Bowman et al. 1998; Jaumé and Sykes 1999; Hainzl et al. 2000; Zöller and Hainzl 2002; Zöller et al. 2002; Chen 2003; Chen and Wu 2006; Wu et al. 2008a, b), the pattern informatics (PI) method is a powerful candidate. Using the PI method, a dynamic pattern prior to a large earthquake can be constructed from observed seismicity (Rundle et al. 2000a, b; Tiampo et al. 2002a).

Some previous studies have investigated precursor activity before a large earthquake using the PI method (Chen et al. 2005; Wu et al. 2008a). Before the occurrence of an earthquake, the hotspots, which will be explained below, can be observed on or around the epicentral area. In addition, anomalous seismicity recognized from the PI map seems to migrate toward the epicenter of an impending earthquake (Wu et al. 2008a). This migration has also been observed in simulated models and rock experiments (Ohnaka and Kuwahara 1990; Rice 1992; Lapusta and Rice 2003). Due to a lack of systematic methods for investigating the temporal variation in earthquake migration patterns in the past, only a few studies (Ando 1975; Mogi 1988) have been conducted.

Wu et al. (2008b) improved the PI method to verify seismic migration. They introduced the self-organizing spinodal (SOS) model to specify related time parameters. Using their modified PI method, time-varying patterns of seismicity can be produced in a progressive series of changing intervals. They observed a decreasing trend in the distances between the PI hotspots and epicenters, and also estimated the slope of the function to approach the decreasing trend. Wu (2010) expanded the technique to two dimensions, with the capability for calculating and imaging the slopes for all grid

---

* Corresponding author
  E-mail: maomao@earth.sinica.edu.tw

sites in a study area. Wu (2010) also identified a donut-like migration pattern where the PI hotspots migrate toward the epicenter in both time and space domains. This approach provides a method to image the nucleation of cracks and accumulation of stresses around the epicenter until the fault breaks.

Seismicity and fault types often show regional dependence due to different tectonic conditions (cf. Isacks et al. 1968). In South California, most earthquakes show strike-slip faulting; while in central Japan, most of the earthquakes show thrust faulting. Compared to earthquakes occurring in southern California and central Japan, the complex tectonic background in Taiwan would make forecasting earthquakes more difficult. Taiwan is located at the junction of the collision zone between the Philippines Sea and Eurasian plates (Seno 1977; Tsai et al. 1977; Wu 1978; Lin 2002). The tectonic conditions in this region are highly complex. Seismicity in Taiwan also shows regional dependence (cf. Wang 1988; Wang et al. 1994). Two large earthquakes, the 1999 M_s 7.6 Chi-Chi earthquake (Ma et al. 1999) and 2006 M_s 7.0 Pingtung earthquake (Ma and Liang 2008), occurred in different tectonic provinces in Taiwan. In this study, we used the 2D PI migration method to measure seismic activities preceding the two earthquake sequences to examine the regional dependence of dynamic patterns of seismicity.

2. METHODOLOGY: PI METHOD AND MIGRA-TION PATTERN MEASUREMENT

According to the concept of pattern dynamics, the PI state vector can show seismicity changes of a system within an interval from t_1 through t_2, following the steps (Rundle et al. 2000a; Tiampo et al. 2002a, b; Chen et al. 2006; Holliday et al. 2007; Wu et al. 2008a, b). The study region and time parameters must be determined first. The time parameters include the beginning of data, t_0, starting point of seismicity change, t_1, and end of seismicity change, i.e., the time just before large earthquake, t_2. The study region is discretized into grid boxes with a size of $0.1° \times 0.1°$, approximately

11 km on a side. The dimension of these boxes corresponds roughly to the linear size of a M ≈ 6 earthquake (Wells and Coppersmith 1994) which could have sufficient influence on the stress and seismicity within the entire box (Nanjo et al. 2006). After dividing the study region into grid boxes of $0.1° \times 0.1°$ in size and evaluating the values of time parameters, the seismic intensity $I(x_i, t_b, t)$, which is defined as the average number of earthquakes with magnitude, M, larger than the cutoff magnitude, M_c, in a grid box x_i and its eight neighboring boxes (so-called the Moore neighbors) during t_b and t, is evaluated. Here, t_b is a sampling reference time that will be shifted from t_0. The seismicity change between t_1 and t_2 is:

$$\Delta I(x_i, t_b, t_1, t_2) = I(x_i, t_b, t_1) - I(x_i, t_b, t_2) \qquad (1)$$

and will be denoted as $\Delta I(x_i, t_b)$ hereafter. To show the change in seismicity, background values are removed through normalization, i.e., subtracting the temporal and spatial means and dividing by their individual standard deviations. Seismic anomalies are shown by positive value for activation and negative values for quiescence. To include the two anomalies in the PI index, we take the absolute value and then estimate its temporal average and mean square. The mean squared change indicates the occurrence probability of future threshold events, so it is plotted as hotspots on a map to show the areas at risk.

To determine whether the hotspots migrate toward the epicenter and to quantify the migration, Wu et al. (2008b) defined the error distance, ε_n, to be the distance between the nth earthquake and the nearest hotspot, as shown in Fig. 1a. They also defined the integrated error distance, $\varepsilon_{area}(t_1)$, to be the area below the curve of the mean error distance $\langle \varepsilon \rangle$ versus coverage ratio f. The coverage ratio f is defined as $f = A_H / A$, where A is the total area of the study region and A_H is the area covered by hotspots. The mean error distance is calculated as

$$\langle \varepsilon \rangle = \frac{1}{N} \sum_{n=1}^{N} \varepsilon_n \qquad (2)$$
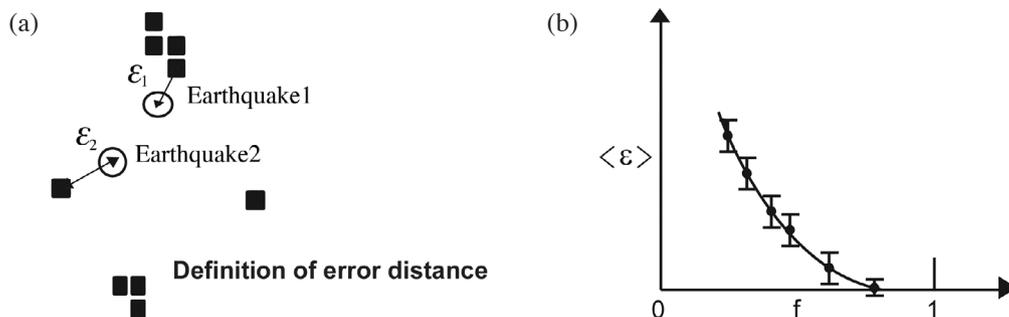
Fig. 1. (a) Schematic diagram of the definition of error distance. The blocks represent the hotspots in a PI map and the circles the locations of large earthquakes occurred after t_2. The error distance ε_n is the distance between the nth earthquake and the hotspot closest to it. (b) The relation between the mean error distance and the coverage fraction f of the PI hotspots.

which varies with the fraction f. Figure 1b shows a decrease in $\langle \varepsilon \rangle$ with increasing f. The decrease is due to the generation of more hotspots in the PI map with a lower threshold, i.e., a higher f. Accordingly, the temporal evolution of anomalous seismic activity on every site can be examined by a plot of $\varepsilon_{area}(t_1)$ versus t_1 as shown in Fig. 2. A site without significant activity, i.e., a lack of hotspot, would have a flat trend, with a slope value close to 0, as in Fig. 2a. When the hotspots spread outwards, the plot (Fig. 2b) shows an increase of $\varepsilon_{area}(t_1)$ with t_1. The related linear regression line will have a positive slope. In contrast, when the locations of the hotspots get closer to a grid, the $\varepsilon_{area}(t_1)$ for the grid will decrease with t_1 and thus have a negative slope value from the curve as Fig. 2c (e.g., Wu et al. 2008b). Therefore, from a 2D map of calculated slope values for all grids, we can visualize the migration of PI hotspots.

3. REGIONAL TECTONICS AND TWO LARGE EARTHQUAKES IN STUDY

In Taiwan, the Philippine Sea plate, which is moving northwestward with a speed of about 8 cm yr^{-1}, collides with the Eurasian plate (Seno 1977; Yu et al. 1997). The Philippine Sea plate has subducted underneath northern Taiwan. However, in southern Taiwan the Eurasian plate moves eastward and subducts underneath the Philippine Sea plate. Detailed descriptions of regional tectonics can be found in Seno 1977; Tsai et al. 1977; Wu 1978; Lin 2002. This collision and subduction cause high seismicity in the Taiwan region (Wang 1998).

On 20 September 1999, the M_s 7.6 Chi-Chi earthquake ruptured the Chelungpu fault, which is a ~100 km long and east-dipping thrust fault, with a dip angle of ~30° in central Taiwan (Ma et al. 1999). The focal depth of the earthquake was ~8 km. The event took place in the collision zone between the Philippine Sea plate and the Eurasian plate. The epicenter was located in the Western Seismic Zone defined by Wu and Chen (2007) where the occurrence of most earthquakes was associated with active faults in the western foothills (Wu and Chen 2007; Wu et al. 2008c). On 26 December 2006, two Pingtung earthquakes, which occurred

about 8 minutes apart, were located offshore southwestern Taiwan (Yen et al. 2008). The focal depths were 44 and 50 km, respectively, for the first and second earthquakes. The focal plane solutions indicated normal faulting for the first event and strike-slip faulting for the second. They occurred in the area where the Eurasian plate starts to subduct eastward beneath the Philippine Sea plate and thus in the Southwestern Seismic Zone defined by Wu and Chen (2007). Most earthquakes in this region have focal depths greater than 30 km with normal-faulting focal mechanisms which are likely associated with the bending of the plunging slab (Wu and Chen 2007; Wu et al. 2008c, 2009). Obviously, the Chi-Chi and Pingtung earthquake sequences took place in different tectonic provinces.

4. DATA

We used the earthquake data from the CWB (Central Weather Bureau) catalogues. Considering the fact that seismic activity preceding a large earthquake usually show observable changes in moderate-sized earthquakes (Jaumé and Sykes 1999) and referring to the results in Wu (2010), only the events with magnitudes larger than 3.7 and 3.2 were selected for the Chi-Chi and Pingtung earthquakes, respectively. The study area ranged from 23.0 to 25.0°N and from 120.0 to 121.5°E for the Chi-Chi earthquake and from 21.0 to 23.0°N and from 119.0 to 121.0°E for the Pingtung earthquake. Note that the latitude of 23°N is quite near the northern edge of the Eurasian plate, which moves eastward and subducts underneath the Philippine Sea plate in southern Taiwan (Tsai 1986; Lin 2002). The focal depths range from 0 to 80 km for the two earthquake sequences. The events in the respective study area are further divided into different groups depending on the depth, e.g., 12 km for Chi-Chi earthquake and 30 km for the Pingtung earthquake, which is regarded as a boundary of seismotectonic setting. We discuss the results of PI maps and migration patterns with different depth ranges for the two earthquakes according to the distribution of focal depth of the mainshocks and the aftershocks. Additional details about the selection criteria are in Wu (2010).
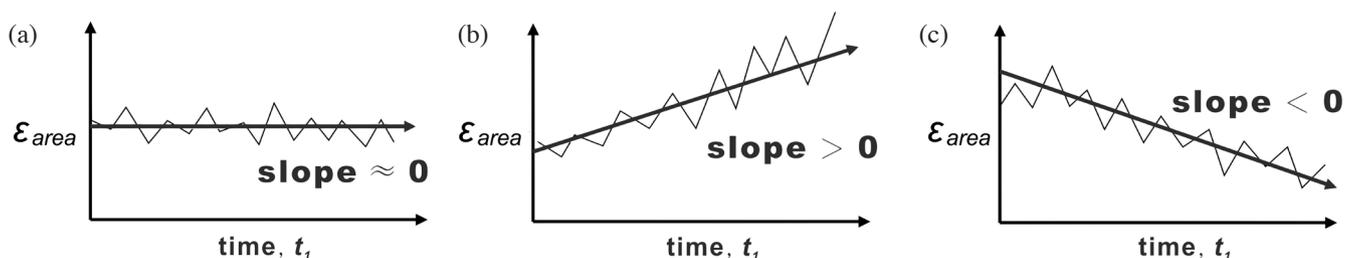
Fig. 2. Integrated error distance $\varepsilon_{area}(t_1)$ obtained by integrating the curve of $\langle \varepsilon \rangle$ versus f. The gray lines indicate the best fit line. The PI hotspots keep in or absent from a site form a smooth trend for $\varepsilon_{area}(t_1)$ with a slope close to 0 as shown in (a), or when the hotspots move away from/close to a site, an increasing/decreasing trend identified by positive/negative slope as in (b)/(c).

5. RESULTS

The temporal variations in $\varepsilon_{area}(t_1)$ using shallower events (0 - 12 km) and deeper events (12 - 80 km) for the Chi-Chi earthquake are shown in Figs. 3a and b, respectively, with t_0 = 1980/01/01, t_2 = 1999/09/20, and t_1 shifting from 1991/01/01 to 1999/01/01 in a unit of three-months. It is clear that $\varepsilon_{area}(t_1)$ decreases for shallower events but increases for deeper events over time. Figure 4 shows the temporal variations in $\varepsilon_{area}(t_1)$ for the Pingtung earthquakes with t_0 = 1990/01/01, t_2 = 2006/12/25, and t_1 shifting from 2000/01/01 to 2006/01/01. Figure 4a shows the shallower events and Fig. 4b shows the deeper events. In contrast to the results of the Chi-Chi earthquake, $\varepsilon_{area}(t_1)$ increases for shallower and decreases for deeper events with time. The linear regression equation is estimated from the data points and displayed by a straight line. For the Chi-Chi earthquake, the slopes of the linear regression lines are about -0.003 km day^{-1} for shallower events and 0.003 km day^{-1} for deeper events. For the Pingtung earthquakes the slopes are 0.008 km day^{-1} for shallower events and -0.006 km day^{-1} for deeper events.

The 2D PI migration maps for the two earthquake sequences in two respective depth ranges were made. On the maps, negative and positive slope values are shown in blue and red, respectively. The maps for the Chi-Chi earthquake, with t_0 = 1980/01/01, t_1 = 1991/01/01 ~ 1999/01/01, and t_2 = 1999/09/20, are shown in Fig. 5: Fig. 5a for shallower events and Fig. 5b for deeper events. In Fig. 5, the epicenter of the Chi-Chi earthquake is denoted by a red star. The maps for the Pingtung earthquakes, with t_0 = 1990/01/01, t_1 = 2000/01/01 ~ 2006/01/01, and t_2 = 2006/12/25, are displayed in Fig. 6, Fig. 6a for shallower events and Fig. 6b for deeper events. In Fig. 6, the epicenters of the Pingtung earthquakes are shown by red stars. Since the PI migration curve shows that the approaching hotspots show a negative slope, the area colored in blue on the PI migration map indicates the area where the directions of hotspots tend to migrate and hence where the anomalous activity is focused. It can be observed that the blue area is very close to the locations of mainshocks when the PI migration is examined within the depth ranges where the mainshocks and their aftershocks occurred or otherwise. The PI migration curve and patterns both show that when only the events within the depth range where the mainshock and aftershocks distributed in are involved in calculation the hotspots migrate toward the hypocenter, otherwise the migration, i.e., the decreasing trend of $\varepsilon_{area}(t_1)$ and hence the negative slope, become ambiguous.

6. DISCUSSION

To make a PI map effectively, it is necessary to select proper data on the basis of model parameters. The model parameters, t_0, t_1, M_c, and depth range, are important factors in constructing the pattern dynamics of an earthquake system. Since the Chi-Chi and Pingtung earthquakes originated from different seismotectonic settings, the pattern dynamics of the earthquake systems are presumed to be different. Thus, different values of model parameters for these two earthquakes should be considered.

A lower bound magnitude (denoted by M_c) of events is used to insure that only moderate events which can indicate precursory activities of the mainshock are involved in PI calculation, thus the M_c might differ from the completeness catalog magnitude. Several researchers (Tiampo et al. 2002a, b; Nanjo et al. 2006; Holliday et al. 2007) used M_c = 3 in the PI calculations for forecasting M > 5 earthquakes. But Taimpo et al. (2002b) found that the value of M_c for earthquakes occurring in South California cannot be applied to other tectonic provinces. From numerical tests, Holliday et al. (2006) found that M_c = 4.5 is the maximum M_c for some tectonic provinces, because they obtained relatively insensitive results when M_c = 3 - 4.5. Wu (2010) found that for earthquakes in Taiwan, the PI hotspots cannot be reliably correlated with the target mainshocks when M_c = 2 - 3 is used. However, when the completeness catalog magnitude, which averages 2.0 using a Maximum Likelihood Estimate (Wiemer 2001; Wu 2010) is taken as M_c, the inferred hotspots can not only indicate the expected locations of the target earthquakes, but also the locations of some smaller earthquakes. Practical tests in Wu (2010) show that M_c is 3.2 for the Pingtung earthquakes and 3.7 for the Chi-Chi earthquake, with these cut magnitudes the number of hotspots is reduced and each hotspot (excluding the hotspots offshore of eastern Taiwan) is almost correlated with the epicenters of the respective events. This suggests that the seismic precursory activity, which is strongly associated with impending large events can be recognized only when moderate earthquakes are taken into account, and the smallest magnitude of those moderate earthquakes increases with the magnitude of the forthcoming large earthquake. In other words, the results from Wu (2010) suggest that such moderate earthquakes should be larger than at least M = 3 when the target earthquake is larger than M = 6.

Since the Chi-Chi earthquake was caused by the collision between the Eurasian and Philippine Sea plates and the Pingtung earthquake was caused by the subduction of the Eurasian plate underneath the Philippines Sea plate, the seismotectonic setting is obviously different. Considering the null-hypothesis that the PI hotspots driven by different pattern dynamics, which are associated with the seismotectonic setting, would present different migration patterns, we selected the study region largely according to Wu and Chen (2007) and the depth range based on the distribution of the mainshock and its aftershocks. Note that the study region for the Chi-Chi earthquake was chosen in consideration of both the tectonic setting and the convenience of calculation and thus included most of the Western Seismic Zone and
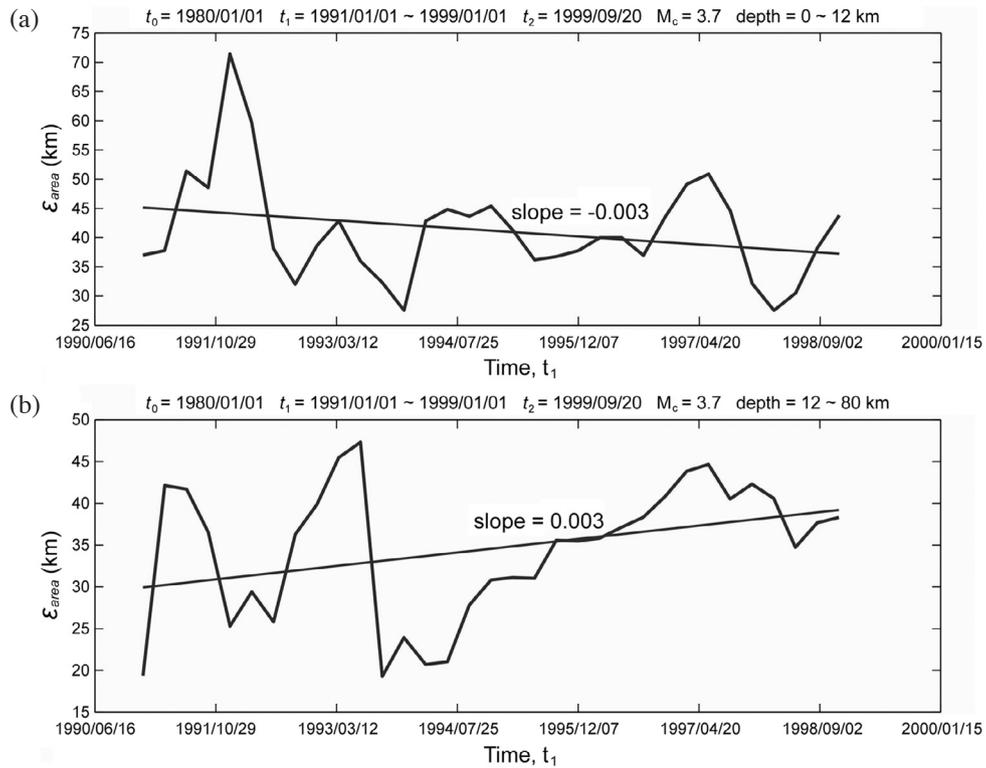
Fig. 3. Integrated error distance $\varepsilon_{area}(t_1)$ and linear fit with $t_0 = 1980/01/01$, $t_1 = 1991/01/01 \sim 1999/01/01$, and $t_2 = 1999/09/20$ for the Chi-Chi earthquake according to a different depth range: (a) 0 - 12 km and (b) 12 - 80 km. A decrease of the integrated error distance in the shallower depth is represented by a negative slope value -0.003, and a positive value 0.003 at a deeper depth.
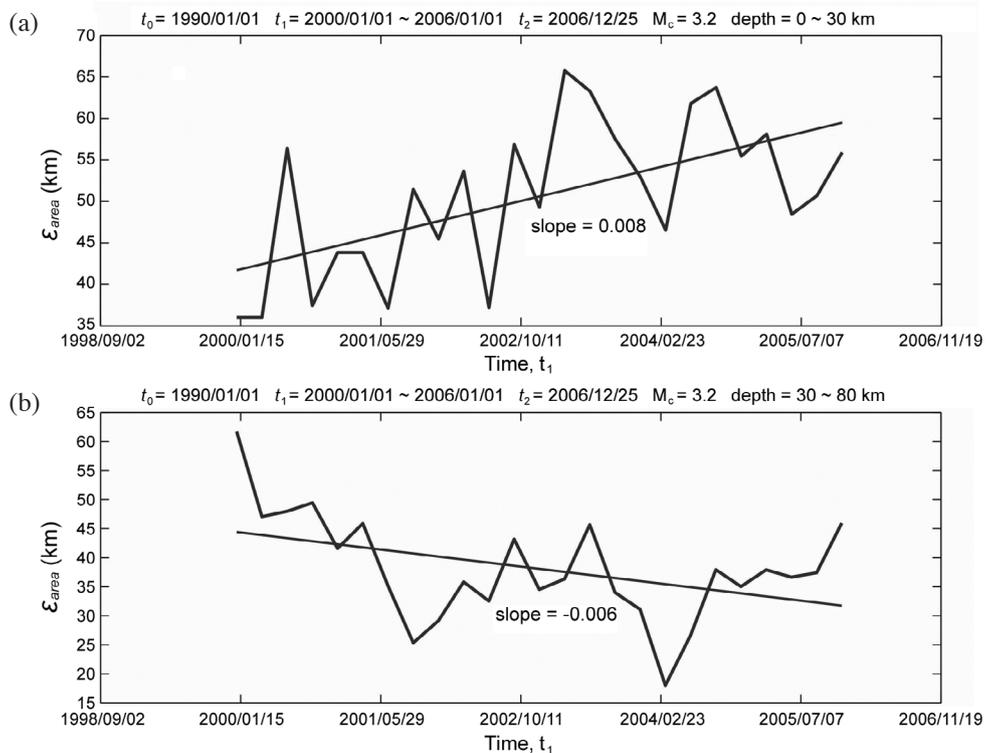
Fig. 4. Integrated error distance $\varepsilon_{area}(t_1)$ with $t_0 = 1990/01/01$, $t_1 = 2000/01/01 \sim 2006/01/01$, and $t_2 = 2006/12/25$ shows an increasing trend and a decreasing trend with the slope value 0.008 and -0.006 in (a) a shallower depth range 0 - 30 km and (b) a deeper depth range 30 - 80 km, respectively, for the Pingtung earthquakes.

(a) t_0=1980/01/01 t_1=1991/01/01~1999/01/01
      t_2=1999/09/20 M_c=3.7 depth=0~12km

(b) t_0=1980/01/01 t_1=1991/01/01~1999/01/01
      t_2=1999/09/20 M_c=3.7 depth=12~80km
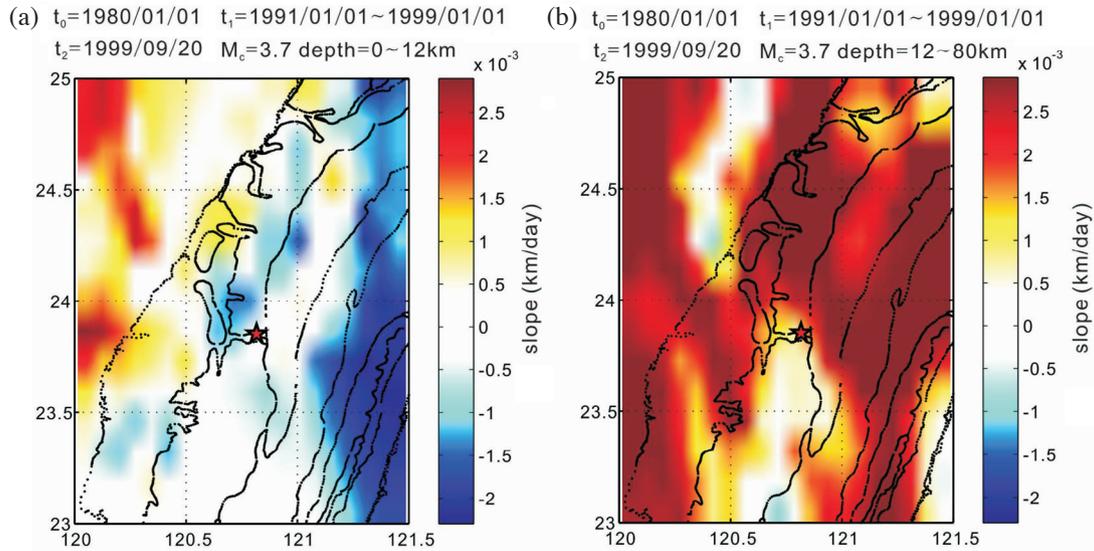
Fig. 5. A 2D migration pattern at (a) 0 - 12 km and (b) 12 - 80 km, for the Chi-Chi earthquake as identified by red star. Negative and positive slope values are shown by blue and red, respectively. The blue shading indicates the area where the hotspots migrate toward.

(a) t_0=1990/01/01 t_1=2000/01/01~2006/01/01
      t_2=2006/12/25 M_c=3.2 depth=0~30km

(b) t_0=1990/01/01 t_1=2000/01/01~2006/01/01
      t_2=2006/12/25 M_c=3.2 depth=30~80km
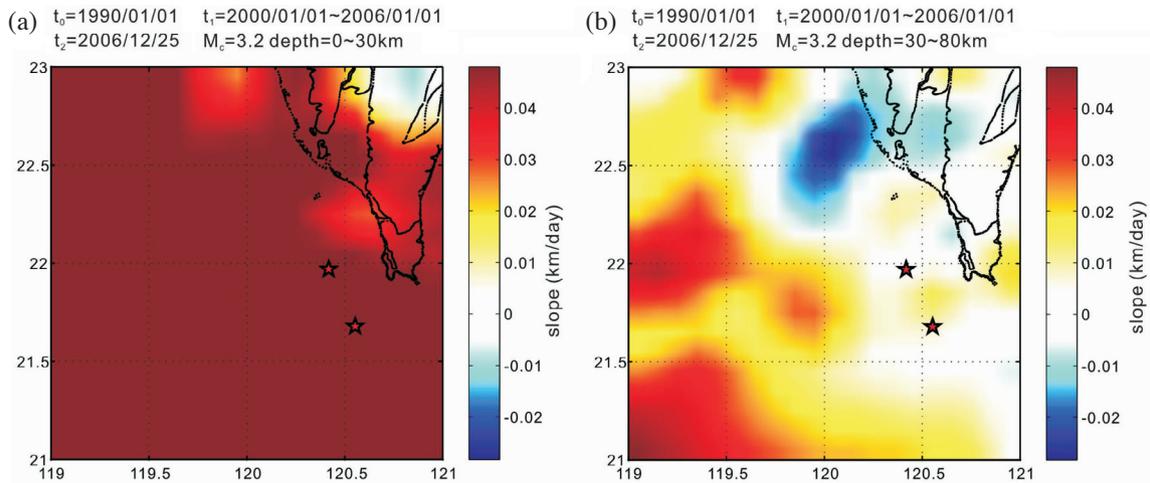
Fig. 6. A 2D migration pattern at depth range (a) 0 - 30 km and (b) 30 - 80 km for the Pingtung earthquake (red star). Negative slopes (blue) can be seen near the epicenter while null (white) and positive (red) slope values appear surrounding the epicentral area.

fractional parts of the Northeastern and Southeastern Seismic Zone in Wu and Chen (2007). From previous studies, we found that the PI results show that hotspots can identify the location of the mainshock only while the events in shallower depth are used for the Chi-Chi earthquake (Chen et al. 2006) and the events in deeper depth are used for the Pingtung earthquake (Wu et al. 2008a). Moreover, the migration of PI hotspots toward the epicentral area only occurs within the appropriate depth range as shown in Figs. 3a and 4b. $\varepsilon_{area}(t_1)$ becomes smaller and smaller as the time approaches the occurrence time of the mainshock. Note that a peak in Fig. 3a occurred in 1992, because some earthquakes occurring near Hualien and Taitung were inevitably involved in the study region. The events which took place

there belong to the Northeastern and Southeastern Seismic Zone which is associated with the subduction and collision of slabs respectively; they were widely distributed in depth (Wu et al. 2008c). The events occurred within the shallow depth in this region cannot be eliminated by depth selection. Therefore, the earthquakes within the boundary of the study region used for the Chi-Chi earthquake contribute to the peak of the migration curve. This result shows that the events in Hualien and Taitung regions are driven by a separate dynamic system from the system of Chi-Chi earthquake sequence since the behavior of the events themselves acts as a kind of noise in the calculation of PI migration for the Chi-Chi earthquake. The slopes of the linear regression lines in Figs. 3a and 4b are -0.003 km day^{-1} for the Chi-Chi earth-

quake and -0.006 km day^{-1} for the Pingtung earthquake. The decreasing trend is statistically significant compared with the result of the stochastic test. After randomly shuffling the occurrence time and the location of catalog for 500 times, the values of the mean slope and the standard deviation as to the two earthquakes are down to 10^{-18} - 10^{-19} and 10^{-19} - 10^{-21}, very close to zero. The stochastic test verifies that the trends we observed from these two cases are not simply statistical fluctuations at the 95% confidence level.

The 2D PI migration patterns show the same characteristic, that is, the migration occurs in their respective seismotectonic zone. In the 2D PI migration patterns (Figs. 5a and 6b) both show that an area surrounded by negative slope values is very close to the epicenter. The distribution of positive values (in red) and almost zero (in white) of slope form a donut-like pattern surrounding that area, indicating that the hotspots migrated toward the location which is near the epicenter. In addition, the epicentral area for the Chi-Chi earthquake was surrounded by negative slope values (see Fig. 5a) when the shallower events with focal depths from 0 to 12 km were considered and surrounded by positive slope values (see Fig. 5b) when the deeper events with focal depths from 12 to 80 km were taken into account. The 2D PI migration maps for the two depth ranges are completely different. The occurrence of the Chi-Chi earthquake was associated with seismicity within the depth range 0 - 12 km but not within the depth range 12 - 80 km. On the other hand, the 2D PI migration map shows a clear migration pattern close to the Pingtung earthquakes (see Fig. 6b) when the shallower events with focal depths from 30 to 80 km were considered and another migration pattern close to Taitung (see Fig. 6a) when the deeper events with focal depths from 0 to 30 km were taken into account. Our results show that the Pingtung earthquakes were associated with seismicity in the focal depth range 30 - 80 km but not with seismicity at depth range 0 - 30 km. Accordingly, the location of an impending earthquake can be recognized from the hotspot inferred from the PI map which is constructed from the events within a proper depth range. As a consequence, it is necessary to separate the earthquakes in the study region into numerous groups with different focal depths to select the most appropriate data for producing the PI map and hence the migration maps.

A significant phenomenon can be observed in Figs. 3a and 4b, that is, the hotspots are closer to the epicentral area of the forthcoming large earthquake when t_1 approaches t_2. Furthermore, the $\varepsilon_{area}(t_1)$ reaches a minimum value of about 2 ~ 3 years before the mainshock followed by a sudden increase. During the crack nucleation processes, seismicity will migrate towards the direction along which the fault grows (Scholz 2002). The slopes in the PI migration pattern are obtained by calculating the motions of the PI hotspots which reflect anomalous seismicity apart from the background seismic signals. We can regard the PI hotspot as a

type of stress meter (Wu et al. 2008b; and Wu 2010). Hence the PI migration pattern shows the precursor processes before the earthquake, including the evolution of the rupture and the accumulation of stress. The migration toward the epicenter, that is, the decrease of the integrated error distance and thus the negative slope, may imply the processes of crack nucleation and stress accumulation. The breaking time of the changing $\varepsilon_{area}(t_1)$ coincides with the phase change from Stage 2 to Stage 3 of the self-organized spinodal model (Rundle et al. 2000c). An increase in moderate-sized events occurred in Stage 2 makes the magnitude-frequency distribution in the form of a power-law, and then a further increase in moderate-sized events which implies seismic activation occurred in Stage 3. The change from Stage 2 to Stage 3 for the Chi-Chi and Pingtung earthquakes is 1998/01/01 and 2004/03/01 respectively (Chen 2003; Wu et al. 2008a), and the integrated error distance stopped decreasing while the moderate-sized events further increase in Stage 3. Moreover, the PI map (Wu et al. 2008b) shows that the hotspots, representing anomalous earthquake activity, remain in the epicentral area in Stage 3. Therefore, the increase of the integrated error distance seems to be associated with the activation in Stage 3 and the activation is related to accelerating seismicity. The preceding decrease of $\varepsilon_{area}(t_1)$ shows the so-called earthquake migration processes (Mogi 1969, 1985; Rydelek and Sacks 2001; Battaglia et al. 2005). These migration processes can be caused by numerous mechanisms. For example, a prominent migration pattern was observed for a series of large earthquakes (M ≥ 7.5) moving down from north to south along the Japan Trench at an interval of 2 or 3 years in the 1930's and was considered indicative of the development of large-scale fracturing along the trench (Mogi 1969, 1985). The appearance of a doughnut pattern formed by earthquakes with M ≥ 3 around the Izu Peninsula was hypothesized by Mogi (1985) as indicating preparation processes prior to the forthcoming large event.

7. CONCLUSIONS

Because complex seismic conditions influence the PI calculations, PI maps work best for forecasting earthquakes when the data and the values of model parameters are selected appropriately. The PI map should be made from the events with particular focal depths and magnitudes larger than M_c. The specific focal depths range from 0 to 12 km for the Chi-Chi earthquake and from 30 to 80 km for the Pingtung earthquakes. M_c was 3.2 for the Pingtung earthquakes and 3.7 for the Chi-Chi earthquake. In addition, seismic precursor activity can be recognized when only moderate earthquakes are taken into account, and the smallest magnitude (i.e., M_c) of the moderate earthquakes increases with the magnitude of the forthcoming large earthquake.

The use of a statistical method in this study allows PI migration before the Chi-Chi and the Pingtung earthquakes

to be identified from the PI maps. The migration of the PI hotspots implies a preparation process before large earthquakes. The duration of these precursor processes can persist for several years, and may increase with the size of impending event. Furthermore, the migration becomes most active when it is close to the mainshock, meaning that the $\varepsilon_{area}(t_1)$ shows the most significant decrease from about 4 - 6 years before to about 2 - 3 years before the mainshock. This migration process might be associated with the nucleation of earthquakes.

The calculation of the slope of the $\varepsilon_{area}(t_1)$ curves expands migration pattern into a 2D map. The 2D PI migration patterns demonstrate a preparation process associated with nucleation before the Chi-Chi and Pingtung earthquakes. Moreover, these patterns show that there are discontinuities at depths of 12 and 30 km in central and southwestern offshore Taiwan, respectively. Totally different patterns above and beneath the critical depth specify the different pattern dynamics. Since the seismotectonic setting is a major factor to influence the pattern dynamics, the earthquakes above and beneath the critical depth belong to different seismotectonic settings.

REFERENCES

Ando, M., 1975: Source mechanisms and tectonic significance of historical earthquakes along the Nankai trough, Japan. *Tectonophysics*, **27**, 119-140, doi: 10.1016/0040-1951(75)90102-X. [Link]

Battaglia, J., V. Ferrazzini, T. Staudacher, K. Aki, and J. L. Cheminée, 2005: Pre-eruptive migration of earthquakes at the Piton de la Fournaise volcano (Réunion Island). *Geophys. J. Int.*, **161**, 549-558, doi: 10.1111/j.1365-246X.2005.02606.x. [Link]

Bowman, D. D., G. Ouillon, C. G. Sammis, A. Sornette, and D. Sornette, 1998: An observational test of the critical earthquake concept. *J. Geophys. Res.*, **103**, 24359-24372, doi: 10.1029/98JB00792. [Link]

Chen, C. C., 2003: Accelerating seismicity of moderate-size earthquakes before the 1999 Chi-Chi, Taiwan, earthquake: Testing time-prediction of the self-organizing spinodal model of earthquakes. *Geophys. J. Int.*, **155**, F1-F5, doi: 10.1046/j.1365-246X.2003.02071.x. [Link]

Chen, C. C. and Y. X. Wu, 2006: An improved region-time-length algorithm applied to the 1999 Chi-Chi, Taiwan earthquake. *Geophys. J. Int.*, **166**, 1144-1148, doi: 10.1111/j.1365-246X.2006.02975.x. [Link]

Chen, C. C., J. B. Rundle, J. R. Holliday, K. Z. Nanjo, D. L. Turcotte, S. C. Li, and K. F. Tiampo, 2005: The 1999 Chi-Chi, Taiwan, earthquake as a typical example of seismic activation and quiescence. *Geophys. Res. Lett.*, **32**, L22315, doi: 10.1029/2005GL023991. [Link]

Chen, C. C., J. B. Rundle, H. C. Li, J. R. Holliday, K. Z. Nanjo, D. L. Turcotte, and K. F. Tiampo, 2006: From tornadoes to earthquakes: Forecast verification for binary events applied to the 1999 Chi-Chi, Taiwan, Earthquake. *Terr. Atmos. Ocean. Sci.*, **17**, 503-516.

Hainzl, S., G. Zöller, J. Kurths, and J. Zschau, 2000: Seismic quiescence as an indicator for large earthquakes in a system of self-organized criticality. *Geophys. Res. Lett.*, **27**, 597-600, doi: 10.1029/1999GL011000. [Link]

Holliday, J. R., J. B. Rundle, K. F. Tiampo, W. Klein, and A. Donnellan, 2006: Systematic procedural and sensitivity analysis of the pattern informatics method for forecasting large (M > 5) earthquake events in southern California. *Pure Appl. Geophys.*, **163**, 2433-2454, doi: 10.1007/s00024-006-0131-1. [Link]

Holliday, J. R., C. C. Chen, K. F. Tiampo, J. B. Rundle, D. L. Turcotte, and A. Donnelan, 2007: A RELM earthquake forecast based on pattern informatics. *Seismol. Res. Lett.*, **78**, 87-93, doi: 10.1785/gssrl.78.1.87. [Link]

Isacks, B., J. Oliver, and L. R. Sykes, 1968: Seismology and the new global tectonics. *J. Geophys. Res.*, **73**, 5855-5899, doi: 10.1029/JB073i018p05855. [Link]

Jaumé, S. C. and L. R. Sykes, 1999: Evolving towards a critical point: A review of accelerating seismic moment/energy release prior to large and great earthquakes. *Pure Appl. Geophys.*, **155**, 279-305, doi: 10.1007/s000240050266. [Link]

Lapusta, N. and J. R. Rice, 2003: Nucleation and early seismic propagation of small and large events in a crustal earthquake model. *J. Goephys. Res.*, **108**, 2205, doi: 10.1029/2001JB000793. [Link]

Lin, C. H., 2002: Active continental subduction and crustal exhumation: The Taiwan orogeny. *Terr. Nova*, **14**, 281-287, doi: 10.1046/j.1365-3121.2002.00421.x. [Link]

Ma, K. F. and W. T. Liang, 2008: Preface to the 2006 Pingtung earthquake doublet special issue. *Terr. Atmos. Ocean. Sci.*, **19**, I-III, doi: 10.3319/TAO.2008.19.6.I(PT). [Link]

Ma, K. F., C. T. Lee, Y. B. Tsai, T. C. Shin, and J. Mori, 1999: The Chi-Chi, Taiwan earthquake: Large surface displacements on an inland thrust fault. *Eos, Trans., AGU*, **80**, 605-611, doi: 10.1029/99EO00405. [Link]

Main, I., 1996: Statistical physics, seismogenesis, and seismic hazard. *Rev. Geophys.*, **34**, 433-462, doi: 10.1029/96RG02808. [Link]

Mogi, K., 1969: Some features of recent seismic activity in and near Japan (2): Activity before and after great earthquakes. *Bull. Earthq. Res. Inst. Tokyo Univ.*, **47**, 395-417.

Mogi, K., 1985: Earthquake Prediction, Academic Press, Tokyo, 355 pp.

Mogi, K., 1988: Downward migration of seismic activity prior to some great shallow earthquakes in Japanese subduction zones - A possible intermediateterm precursor. *Pure Appl. Geophys.*, **126**, 447-463, doi: 10.1007/BF00879006. [Link]

Nanjo, K. Z., J. R. Holliday, C. C. Chen, J. B. Rundle, and D. L. Turcotte, 2006: Application of a modified pattern informatics method to forecasting the locations of future large earthquakes in the central Japan. *Tectonophysics*, **424**, 351-366, doi: 10.1016/j.tecto.2006.03.043. [Link]

Ohnaka, M. and Y. Kuwahara, 1990: Characteristic features of local breakdown near a crack-tip in the transition zone from nucleation to unstable rupture during stick-slip shear failure. *Tectonophysics*, **175**, 197-220, doi: 10.1016/0040-1951(90)90138-X. [Link]

Rice, J. R., 1992: Dislocation nucleation from a crack tip: An analysis based on the Peierls concept. *J. Mech. Phys. Solids*, **40**, 239-271, doi: 10.1016/S0022-5096(05)80012-2. [Link]

Rundle, J. B., W. Klein, K. F. Tiampo, and S. Gross, 2000a: Linear pattern dynamics in nonlinear threshold systems. *Phys. Rev. E*, **61**, 2418-2431, doi: 10.1103/PhysRevE.61.2418. [Link]

Rundle, J. B., W. Klein, S. Gross, and K. F. Tiampo, 2000b: Dynamics of seismicity patterns in systems of earthquake faults. In: Rundle, J. B., D. L. Turcotte, and W. Klein (Eds.), Geocomplexity and the Physics of Earthquakes. Am. Geophys. Union., Washington DC, 127-146.

Rundle, J. B., W. Klein, D. L. Turcotte, and B. D. Malamud, 2000c: Precursory seismic activation and critical-point phenomena. *Pure Appl. Geophys.*, **157**, 2165-2182, doi: 10.1007/PL00001079. [Link]

Rydelek, P. A. and I. S. Sacks, 2001: Migration of large earthquakes along the San Jacinto Fault; Stress diffusion from the 1857 Fort Tejon Earthquake. *Geophys. Res. Lett.*, **28**, 3079-3082, doi: 10.1029/2001GL013005. [Link]

Scholz, C. H., 2002: The Mechanics of Earthquakes and Faulting, 2nd Edition, Cambridge University Press, Cambridge, UK, 471 pp.

Seno, T., 1977: The instantaneous rotation vector of the Philippine sea plate relative to the Eurasian plate. *Tectonophysics*, **42**, 209-226, doi: 10.1016/0040-1951(77)90168-8. [Link]

Tiampo, K. F., J. B. Rundle, S. McGinnis, S. J. Gross, and W. Klein, 2002a: Mean-field threshold systems and phase dynamics: An application to earthquake fault systems. *Europhys. Lett.*, **60**, 481-487, doi: 10.1209/epl/i2002-00289-y. [Link]

Tiampo, K. F., J. B. Rundle, S. J. McGinnis, and W. Klein, 2002b: Pattern dynamics and forecast methods in seismically active regions. *Pure Appl. Geophys.*, **159**, 2429-2467, doi: 10.1007/s00024-002-8742-7. [Link]

Tsai, Y. B., 1986: Seismotectonics of Taiwan. *Tectonophysics*, **125**, 17-37, doi: 10.1016/0040-1951(86)90005-3. [Link]

Tsai, Y. B., T. L. Teng, J. M. Chiu, and H. L. Liu, 1977: Tectonic implications of the seismicity in the Taiwan region. *Mem. Geol. Soc. China*, **2**, 13-41.

Wang, J. H., 1988: b values of shallow earthquakes in Taiwan. *Bull. Seismol. Soc. Am.*, **78**, 1243-1254.

Wang, J. H., 1998: Studies of earthquake seismology in Taiwan during the 1897-1996 period. *J. Geol. Soc. China*, **41**, 291-336.

Wang J. H., 2008: One-dimensional dynamical modeling of earthquakes: A review. *Terr. Atmos. Ocean. Sci.*, **19**, 183-203, doi: 10.3319/TAO.2008.19.3.183(T). [Link]

Wang, J. H., K. C. Chen, and T. Q. Lee, 1994: Depth distribution of shallow earthquakes in Taiwan. *J. Geol. Soc. China*, **37**, 125-142.

Wiemer, S., 2001: A software package to analyze seismicity: ZMAP. *Seismol. Res. Lett.*, **72**, 373-382.

Wu, F. T., 1978: Recent tectonics of Taiwan. *J. Phys. Earth*, **26 (Suppl.)**, S265-S299.

Wu, Y. H., 2010: Precursory seismicity patterns examined by improved pattern informatics method. Ph.D. Dissertation, National Central University, 112 pp.

Wu, Y. H., C. C. Chen, and J. B. Rundle, 2008a: Precursory seismic activation of the Pingtung (Taiwan) offshore doublet earthquakes on 26 December 2006: A pattern informatics analysis. *Terr. Atmos. Ocean. Sci.*, **19**, 743-749, doi: 10.3319/TAO.2008.19.6.743(PT). [Link]

Wu, Y. H., C. C. Chen, and J. B. Rundle, 2008b: Detecting precursory earthquake migration patterns using the pattern informatics method. *Geophys. Res. Lett.*, **35**, L19304, doi: 10.1029/2008GL035215. [Link]

Wu, Y. M. and C. C. Chen, 2007: Seismic reversal pattern for the 1999 Chi-Chi, Taiwan, M_w 7.6 earthquake. *Tectonophysics*, **429**, 125-132, doi: 10.1016/j.tecto.2006.09.015. [Link]

Wu, Y. M., L. Zhao, C. H. Chang, and Y. J. Hsu, 2008c: Focal-mechanism determination in Taiwan by genetic algorithm. *Bull. Seismol. Soc. Am.*, **98**, 651-661. doi: 10.1785/0120070115. [Link]

Wu, Y. M., L. Zhao, C. H. Chang, N. C. Hsiao, Y. G. Chen, and S. K. Hsu, 2009: Relocation of the 2006 Pingtung Earthquake sequence and seismotectonics in Southern Taiwan. *Tectonophysics*, **479**, 19-27, doi: 10.1016/j.tecto.2008.12.001. [Link]

Yen, Y. T., K. F. Ma, and Y. Y. Wen, 2008: Slip partition of the 26 December 2006 Pingtung, Taiwan (M 6.9, M 6.8) earthquake doublet determined from teleseismic waveforms. *Terr. Atmos. Ocean. Sci.*, **19**, 567-578, doi: 10.3319/TAO.2008.19.6.567(PT). [Link]

Yu, S. B., H. Y. Chen, and L. C. Kuo, 1997: Velocity field of GPS stations in the Taiwan area. *Tectonophysics*, **274**, 41-59, doi: 10.1016/S0040-1951(96)00297-1. [Link]

Zöller, G. and S. Hainzl, 2002: A systematic spatiotemporal test of the critical point hypothesis for large earthquakes. *Geophys. Res. Lett.*, **29**, 1558, doi: 10.1029/2002GL014856. [Link]

Zöller, G., S. Hainzl, J. Kurths, and J. Zschau, 2002: A systematic test on precursory seismic quiescence in Armenia. *Nat. Hazards*, **26**, 245-263, doi: 10.1023/A:1015685006180. [Link]